# Cdc42 interacting protein 4 (CIP4) is essential for integrin-dependent T-cell trafficking

Suresh Koduru[a], Lalit Kumar[a], Michel J. Massaad[a], Narayanaswamy Ramesh[a], Séverine Le Bras[a], Esra Ozcan[a], Michiko K. Oyoshi[a], Mayumi Kaku[b], Yuko Fujiwara[b], Leonor Kremer[c], Sandra King[d], Robert Fuhlbrigge[a,d], Scott Rodig[e], Peter Sage[f], Chris Carman[f], Pilar Alcaide[g], Francis W. Luscinskas[g], and Raif S. Geha[a,h,1]

Divisions of [a]Immunology and [b]Hematology, Children's Hospital, Boston, MA 02115; [c]Department of Immunology and Oncology, Centro Nacional de Biotecnologia-Consejo Superior de Investigaciones Cientificas, E-28049 Madrid, Spain; Departments of [d]Dermatology and [e]Pathology, Brigham and Women's Hospital, Boston, MA 02115; [f]Center for Vascular Biology Research, Beth Israel Deaconess Medical Center, Boston, MA 02115; [g]Center for Excellence in Vascular Biology, Brigham and Women's Hospital, Boston, MA 02115; and [h]Departments of Pediatrics, Dermatology, Pathology, and Medicine, Harvard Medical School, Boston, MA 02115

Edited* by Jack Strominger, Harvard University, Cambridge, MA, and approved August 10, 2010 (received for review March 3, 2010)

**The F-BAR domain containing protein CIP4 (Cdc42 interacting protein 4) interacts with Cdc42 and WASP/N-WASP and is thought to participate in the assembly of filamentous actin. CIP4$^{-/-}$ mice had normal T- and B-lymphocyte development but impaired T cell-dependent antibody production, IgG antibody affinity maturation, and germinal center (GC) formation, despite an intact CD40L–CD40 axis. CIP4$^{-/-}$ mice also had impaired contact hypersensitivity (CHS) to haptens, and their T cells failed to adoptively transfer CHS. Ovalbumin-activated CD4$^{+}$ effector T cells from CIP4$^{-/-}$/OT-II mice migrated poorly to antigen-challenged skin. Activated CIP4$^{-/-}$ T cells exhibited impaired adhesion and polarization on immobilized VCAM-1 and ICAM-1 and defective arrest and transmigration across murine endothelial cell monolayers under shear flow conditions. These results demonstrate an important role for CIP4 in integrin-dependent T cell-dependent antibody responses and GC formation and in integrin-mediated recruitment of effector T cells to cutaneous sites of antigen-driven immune reactions.**

F-BAR | inflammation | contact hypersensitivity | antigen response | adhesion

CIP4 (Cdc42 interacting protein 4) is a member of the Fes–CIP4 homology-Bin/Amphyphysin/Rvsp (F-BAR) family of proteins, which includes FBP17 (formin binding protein 17) and Toca-1 (transducer of Cdc42-dependent actin assembly 1) (1). CIP4 interacts with Cdc42 and is a downstream target of activated GTP-bound Cdc42 (2). The structure of Pombe Cdc 15 homology (PCH) family members consists of a highly conserved N-terminal FCH (Fer-CIP4 homology) domain, followed by two central coiled-coil motifs and a C-terminal SH3 domain. The combination of the FCH domain and first coiled-coil motif is termed F-BAR/EFC (F-BAR/extended FC). The F-BAR domain binds phospholipids in the lipid membrane, the F-BAR/EFC domain interacts with microtubules, the second coiled-coil motif associates with small Rho family GTPases, and the C-terminal SH3 domain interacts with Wiskott-Aldrich syndrome protein (WASP) and WASP-family verprolin-homologous protein (WAVE) (3).

By binding to membrane phospholipids and to Cdc42, WASP/N-WASP and WAVE, F-BAR domain-containing proteins recruit the actin polymerizing machinery to drive membrane curvature, which is important for cytokinesis, cell motility, and endocytosis (4). CIP4 knockdown in HeLa cells interferes with vesicle trafficking (5). A role for CIP4 in endocytosis and in insulin-stimulated Glut4 translocation and glucose uptake has been recently demonstrated in CIP4 knockout mice (6). CIP4 links microtubules to WASP, and both molecules are important for the formation of podosomes (7).

The adaptive immune response requires transendothelial migration (TEM) of leukocytes into lymphoid tissues where critical interactions occur between immune cells and into sites of antigen invasion. This involves a multistep adhesion cascade including tethering and rolling on endothelial surfaces, mediated by interaction between selectin ligands on leukocytes and endothelial selectins, followed by chemokine-driven firm adhesion (arrest), mediated by the interaction of activated β1 and β2 integrins on leukocytes and their ligands on endothelial cells, and finally TEM (8). TEM of leukocytes involves membrane deformation and is dependent on WASP (9). Because CIP4 is involved in membrane deformation and interacts with WASP, we generated CIP4$^{-/-}$ mice to examine its role in lymphocyte function.

## Results

**Generation of CIP4$^{-/-}$ Mice.** CIP4 mRNA is expressed by a wide variety of tissues (1). We confirmed CIP4 protein expression in mouse spleen, thymus, splenic T cells, CD4$^{+}$ T cells, bone marrow-derived dendritic cells (BMDC), and B cells (Fig. S1*A*). The strategy to generate CIP4$^{-/-}$ mice is depicted in Fig. S1 *B–E*. Western blotting of lung lysates from CIP4$^{-/-}$ mice revealed no detectable CIP4 protein (Fig. S1*F*). CIP4$^{-/-}$ mice did not display apparent differences from wild-type (WT) littermates. All experiments were performed on CIP4$^{-/-}$ mice backcrossed into the C57BL/6 background for at least seven generations.

**Normal Lymphoid Development and in Vitro T- and B-Cell Function in CIP4$^{-/-}$ Mice.** Bone marrow, thymus, spleen, and lymph node (LN) cellularity was normal in CIP4$^{-/-}$ mice. FACS analysis revealed no significant differences in the percentages of CD4$^{+}$ and CD8$^{+}$ cells in thymus; CD3$^{+}$, B220$^{+}$, CD4$^{+}$, CD8$^{+}$ cells in spleen, and CD4$^{+}$/Foxp3$^{+}$ cells in thymus, blood, and spleen from CIP4$^{-/-}$ and WT controls (Fig. S2 *A* and *B*). Bone marrow subpopulations of pro- and pre-B cells, immature B cells, and mature B cells were comparable (Fig. S2*A*).

Purified CD3$^{+}$ splenic T cells from CIP4$^{-/-}$ mice and WT littermates were comparable in their ability to proliferate in response to plate-coated anti-CD3 (Fig. S3*A*), secrete IL-2, IFN-γ, and IL-4 in response to anti-CD3 + anti-CD28 (Fig. S3*B*), and up-regulate surface expression of CD40L (Fig. S3*C*). The survival of CD3$^{+}$ T cells from CIP4$^{-/-}$ and WT mice in anti-CD3 stimulated cultures was comparable as assessed by annexin V staining (Fig. S3*D*). Baseline cellular F-actin content, and F-actin increase after anti-CD3 stimulation were comparable in CIP4$^{-/-}$

Author contributions: S. Koduru, L. Kumar, R.F., C.C., F.W.L., and R.S.G. designed research; S. Koduru, L. Kumar, M.J.M., N.R., S.L., E.O., M.K.O., M.K., Y.F., S. King, P.S., and P.A. performed research; L. Kremer contributed new reagents/analytic tools; S. Koduru, L. Kumar, M.J.M., N.R., M.K.O., S. King, R.F., S.R., P.S., C.C., P.A., F.W.L., and R.S.G. analyzed data; and S. Koduru and R.S.G. wrote the paper.

The authors declare no conflict of interest.

*This Direct Submission article had a prearranged editor.

[1]To whom correspondence should be addressed. E-mail: raif.geha@childrens.harvard.edu.

This article contains supporting information online at www.pnas.org/lookup/suppl/doi:10.1073/pnas.1002747107/-/DCSupplemental.

and WT T cells (Fig. S3*E*). CIP4$^{-/-}$ T cells capped CD3 normally after ligation with anti-CD3 (Fig. S3*F*) and spread normally over anti-CD3 coated plates (Fig. S3*G*) with 80 ± 9% spread cells in CIP4$^{-/-}$ vs. 87 ± 8% in WT. Purified B cells from CIP4$^{-/-}$ mice proliferated normally in response to anti-CD40, anti-IgM mAb, and lipopolysaccharide (LPS) (Fig. S3*H*), and secreted normal amounts of IgG1 in response to LPS + IL-4 and anti-CD40 + IL-4 (Fig. S3*I*). The in vitro cytolytic activity of splenic CD8$^+$ T cells and NK cells against allogeneic targets and Yac-1 targets, respectively, was comparable in CIP4$^{-/-}$ mice and WT controls (Fig. S4 *A* and *B*).

**Impaired T-Dependent (TD) Antibody Response in CIP4$^{-/-}$ Mice.** Serum levels of immunoglobulins were comparable in CIP4$^{-/-}$ mice and WT littermates (Fig. S5*A*). CIP4$^{-/-}$ mice mounted normal IgM and IgG anti-TNP responses to the T-independent (TI) antigens TNP–LPS and TNP–Ficoll (Fig. S5 *B* and *C*). CIP4$^{-/-}$ mice mounted a normal IgM antibody response to the TD antigen KLH. In contrast, their anti-KLH IgG and IgE responses were significantly decreased (Fig. 1*A*).

T cell-dependent isotype switching requires T-cell secretion of cytokines, expression of CD40L, and GC formation (10). Following KLH stimulation, splenocytes from immunized CIP4$^{-/-}$ mice and WT controls showed comparable proliferation (Fig. 1*B*), and secretion of INF-γ and IL-4, which direct switching to IgG2a and to IgG1 and IgE, respectively (Fig. 1*C*). Staining of spleens with peanut agglutinin (PNA) revealed that GCs were less numerous and less prominent in CIP4$^{-/-}$ mice than WT controls (Fig. 1*D*), but the density of CD3$^+$ cells in the GCs was comparable (0.00138 ± 0.00096 in CIP4$^{-/-}$ vs. 0.00124 ± 0.00050/μm$^2$ in WT). The percentage of B220$^+$IgD$^{lo}$Fas$^+$GL7$^+$ GC B cells in the spleen was significantly lower in TNP–KLH immunized CIP4$^{-/-}$ mice than WT controls (Fig. 1*E*). The GC reaction is essential for somatic hypermutation and generation of high-affinity antibodies (10). CIP4$^{-/-}$ mice immunized with TNP–KLH mounted a significantly lower IgG anti-TNP response, with a significantly lower affinity to TNP than WT mice (Fig. 1 *F* and *G*).

**Impaired Contact Hypersensitivity (CHS) in CIP4$^{-/-}$ Mice.** CHS is a prototype of an effector T cell-dependent in vivo immune function (11). CIP4$^{-/-}$ mice sensitized with oxazalone (OXA) developed significantly less ear swelling, markedly less cellular infiltration and edema, and significantly lower IFN-γ, but not IL-4, mRNA expression compared with WT controls (Fig. 2 *A*–*C*). CIP4$^{-/-}$ mice had impaired CHS to another hapten, 2,4-dinitrofluorobenzene (Fig. S6). The failure of CIP4$^{-/-}$ mice to mount CHS did not result from failure to mobilize skin DCs to draining LN (DLN). Twenty-four hours after painting the skin with the hapten FITC, the numbers of FITC$^+$ DCs in DLN were comparable in CIP4$^{-/-}$ and WT mice (Fig. S7*A*). DCs from CIP4$^{-/-}$ mice and WT controls were comparable in their ability to present antigen to CD4$^+$ T cells (Fig. S7*B*).

To examine whether defective CHS in CIP4$^{-/-}$ mice involved an intrinsic T cell defect, we compared the ability of cells from skin DLN of OXA-sensitized CIP4$^{-/-}$ and WT donors to adoptively transfer CHS. LN cells from WT donors conferred on CIP4$^{-/-}$ recipients the ability to mount CHS. In contrast, LN cells from CIP4$^{-/-}$ donors failed to confer on WT recipients the ability to mount CHS (Fig. 2 *D* and *E*). Following OXA sensitization, there was a comparable rise in the percentage of CD4$^+$CD44$^{hi}$CD62L$^{lo}$CCR7$^-$ effector memory T cells in DLN from CIP4$^{-/-}$ and WT donors (Fig. S7 *C* and *D*). Furthermore, following i.p. immunization with OVA of CIP4$^{-/-}$/OT-II and WT/OT-II transgenic mice there was a comparable increase in the percentage of splenic effector memory T cells that express both Vα2 and Vβ5 T cell receptor (TCR) chains used by the OT-II transgenic TCR (Fig. S7 *E* and *F*), suggesting that the generation of antigen-specific T effector cells was intact in CIP4$^{-/-}$ mice.

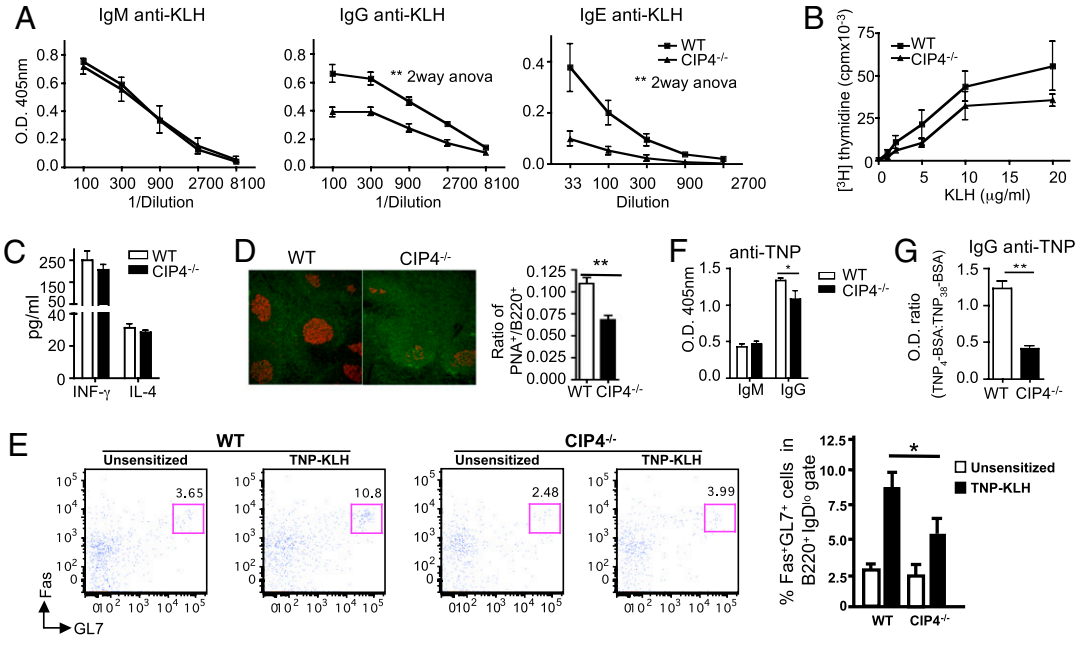


**Fig. 1.** T- and B-cell responses to TD antigen in CIP4$^{-/-}$ mice. (*A*) KLH-specific serum antibody responses. (*B* and *C*) Proliferation (*B*) and cytokine secretion (*C*) by splenocytes in response to KLH. Cytokine secretion in medium was <1 pg/mL for IFN-γ and undetectable for IL-4. (*D*) Staining of spleen sections from KLH immunized mice for PNA (red) and B220 (green) at magnification 200× and ratio of PNA$^+$/B220$^+$ areas (10–15 fields/spleen). (*E*) Representative FACS analysis and mean percentage of Fas$^+$GL7$^+$ GC B cells among B220$^+$IgD$^{lo}$ cells in TNP–KLH immunized mice. (*F* and *G*) TNP-specific IgM and IgG antibody response to immunization with TNP–KLH and affinity maturation of IgG antibodies in mice immunized with TNP–KLH. Sera were used at 1:3,000 dilution. Data are from eight mice per group in *A*, three to four in *B*–*E*, and six in *F* and *G*. *$P < 0.05$, **$P < 0.01$.

IMMUNOLOGY

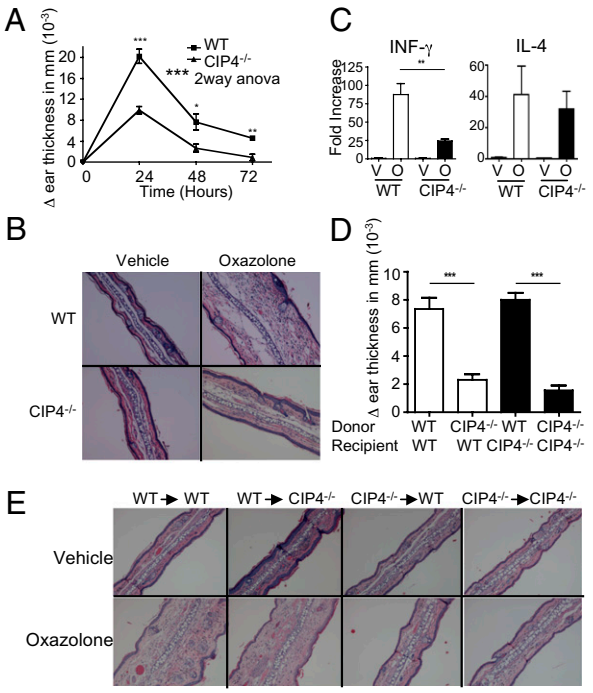


**Fig. 2.** CHS defect in CIP4$^{-/-}$ mice are T-cell intrinsic. (*A*) Ear swelling: difference in thickness between OXA- and vehicle-challenged ears ($n$ = 11 per group). (*B*) Representative ear skin histology 24 h postchallenge. 100× magnification. (*C*) IFN-γ and IL-4 mRNA expression as fold increase in OXA-challenged (O) over vehicle-challenged (V) ears ($n$ = 5 per group). (*D* and *E*) Swelling (*D*) and representative skin histology (*E*) of hapten vs. vehicle-challenged ears of recipients ($n$ = 15 each) of LN cells from OXA-sensitized WT and CIP4$^{-/-}$ donors. Error bars represent mean ± SEM. $^{**}P < 0.01$, $^{***}P < 0.0001$.

**Impaired Accumulation of CIP4$^{-/-}$ Effector T Cells in Antigen-Challenged Skin.** To test the hypothesis that CIP4 might be important for skin homing of effector T cells, we examined the capacity of OVA-activated splenic CD4$^+$ T cells from CIP4$^{-/-}$/OT-II mice to accumulate in OVA-challenged skin sites. CD4$^+$ T cells from CIP4$^{-/-}$/OT-II mice and WT/OT-II controls exhibited comparable proliferation, survival, secretion of INF-γ and IL-4, and expression of the skin homing receptors E-selectin ligands and CCR4 in response to in vitro stimulation with OVA (Fig. 3 *A*–*C*). Thy1.1$^+$ WT recipients of OVA-activated CD4$^+$ T cells from Thy1.2$^+$ CIP4$^{-/-}$ and WT donors were challenged by intradermal (i.d.) injection in ears of OVA + incomplete Freund's adjuvant (IFA) or saline + IFA as control. Seven days later, CD4$^+$Thy1.2$^+$ cells from WT donors accumulated significantly more in OVA-challenged ears than in saline-challenged ears (Fig. 3 *D* and *E*). T cells from CIP4$^{-/-}$ donors accumulated significantly less (~10-fold less) in OVA-challenged ears than CD4$^+$ T cells from WT donors (Fig. 3 *D* and *E*), suggesting that CIP4 is important for the homing of effector CD4$^+$ T cells to cutaneous sites of antigen challenge. Similar results were obtained when tape-stripped ear skin was challenged by painting with OVA + cholera toxin (Fig. S8), although accumulation of WT T cells in this model was less.

**Defective Adhesion to Integrin Ligands and Endothelial Cells and Impaired TEM of CIP4$^{-/-}$ T Cells.** Expression of L-selectin (CD62L), the L-selectin ligand CD44, and E-selectin ligands on CD4$^+$ T cells was comparable in CIP4$^{-/-}$ and WT mice (Fig. S9*A* and Fig. 3*C*). CIP4$^{-/-}$ T cells tethered and rolled normally on immobilized E-selectin and P-selectin under shear flow conditions, and their rate of detachment with increasing levels of shear flow was comparable to that of WT T cells (Fig. S9*B*). CIP4$^{-/-}$ T cells expressed normal amounts of CXCR4, the receptor for the chemokine SDF-1α, and migrated normally after 2 h across 5-μM filters toward SDF-1α (Fig. S9*C*). In addition, CIP4$^{-/-}$ T cells expressed normal levels of the integrins LFA-1 (αLβ2), and VLA-4 (α4β1), which mediate adhesion to ICAM-1 and VCAM-1, respectively (Fig. 4*A*). Anti-CD3 stimulation caused a comparable increase in the adhesion of CIP4$^{-/-}$ and WT T cells to ICAM-1–coated wells, indicating that CIP4 is not essential for TCR/CD3-driven LFA-1 activation (Fig. S9*D*). Furthermore anti-CD3 activated CIP4-deficient CD4$^+$ T cells exhibited intact directional chemotaxis on plates coated with ICAM-1 and SDF-1α (Fig. S9*E*). To assess integrin-dependent adhesion and migration under static conditions, we examined the migration of OVA-activated CD4$^+$ OT-II cells after 30 min toward SDF-1α across ICAM-1–coated 3-μM filters (12). Migration of WT T cells across ICAM-1–coated filters was substantially enhanced compared with migration across uncoated filters, demonstrating that LFA1–ICAM-1 interactions play an important role in this short-term assay (Fig. 4*B*). Migration of OVA activated CIP4$^{-/-}$ T cells toward SDF-1α was comparably enhanced by coating the filters with ICAM-1.

Recruitment of effector T cells to sites of immune reaction or inflammation requires integrin-mediated arrest and TEM under shear flow conditions. Th1 polarized CD4$^+$ T cells from CIP4$^{-/-}$ and WT mice were examined for their adhesive interactions with immobilized VCAM-1 and ICAM-1 under physiological flow conditions (1–2 dyne/cm$^2$). Most WT Th1 cells arrested, and a low percentage rolled on VCAM-1. In contrast, significantly fewer CIP4$^{-/-}$ Th1 cells adhered to VCAM-1 and most of them tethered and rolled (Fig. 4*C*). Differential interference contrast (DIC) microscopy revealed that most WT Th1 cells were arrested and polarized, forming uropods and pseudopods (Fig. 4*C*

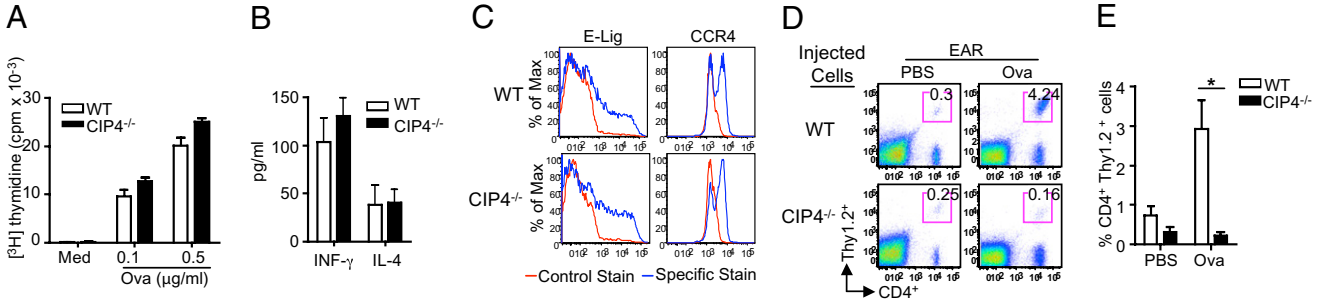


**Fig. 3.** Defective trafficking of CIP4$^{-/-}$ T cells to skin. (*A*) Proliferation. (*B*) Cytokine secretion. (*C*) Expression of E-selectin ligand (lig) and CCR4 on OT-II CD4$^+$ T cells from WT and CIP4$^{-/-}$ mice following stimulation with OVA peptide and DCs from WT mice. Cytokine secretion in medium was as in Fig. 1C. (*D*) Representative FACS analysis of CD4$^+$ Thy1.2$^+$ donor cells from WT and CIP4$^{-/-}$ mice in challenged ears of Thy1.1$^+$ WT recipients. (*E*) Numbers of CD4$^+$ Thy1.2$^+$ donor cells in recipient ears ($n$ = 3 each group). Error bars represent mean ± SEM. $^*P < 0.05$.

and Movie S1). In contrast, most CIP4$^{-/-}$ Th1 cells were rolling and had a rounded shape, and only a few of those that arrested were polarized (Fig. 4*C* and Movie S2). CIP4$^{-/-}$ Th1 cells also adhered significantly less to ICAM-1–coated surfaces (Fig. 4*D*). DIC imaging revealed most WT Th1 cells to be polarized with a flattened and spread shape (Fig. 4*D* and Movie S3). CIP4$^{-/-}$ Th1 cells were less numerous per field and poorly polarized (Fig. 4*D* and Movie S4).

We directly examined the capacity of CIP4$^{-/-}$ Th1 cells to arrest and migrate across a TNF-α activated murine endothelial cell monolayer under physiological low flow conditions (0.8 dyne/cm$^2$). CIP4$^{-/-}$ Th1 cells adhered significantly less to the monolayer, and the percentage of rolling CIP4$^{-/-}$ Th1 cells was significantly greater than that of WT Th1 cells (Fig. 4*E*). DIC microscopy revealed that most WT Th1 cells were arrested and polarized, and subsequently 20–25% of arrested cells transmigrated (Fig. 4*E* and Movie S5). In contrast, most CIP4$^{-/-}$ Th1 cells were rolling, and only a few of those that arrested were polarized. More importantly, the fraction of adherent cells that transmigrated across the endothelial monolayer was significantly lower for CIP4$^{-/-}$ cells compared with WT cells (Fig. 4*E* and Movie S6).

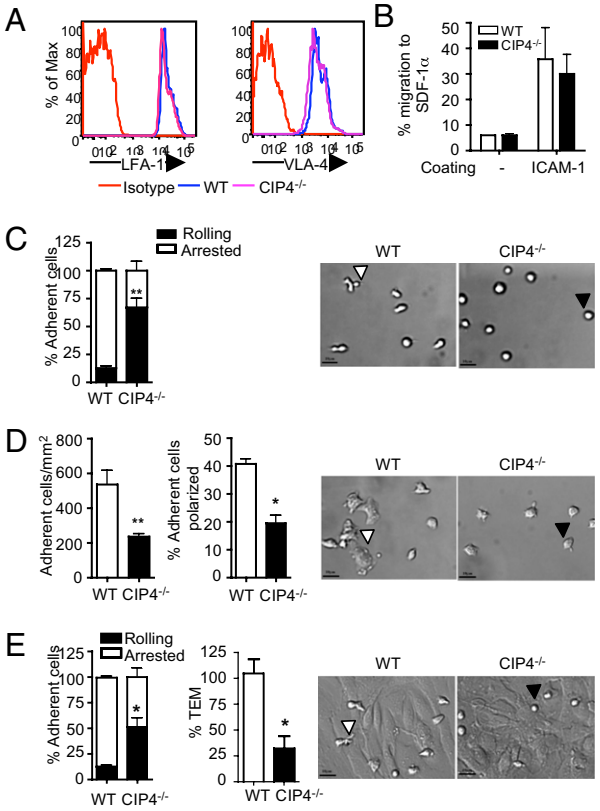


**Fig. 4.** Defective adhesion to VCAM-1 and ICAM-1 and impaired TEM of T cells from CIP4$^{-/-}$ mice. (*A*) LFA-1 and VLA-4 expression by CD4$^+$ T cells (representative of three independent experiments). (*B*) Chemotaxis of OVA-activated OT-II CD4$^+$ T cells to SDF-1α across 3-μM pore filters with or without ICAM-1 coating ($n = 3$). (*C* and *D*) Th1 cells arrest and rolling over VCAM-1 (*C*) and arrest and polarization over ICAM-1 (*D*) under 1 dyne/cm$^2$ shear force. Similar results were obtained under 2 dyne/cm$^2$ shear force. (*E*) Th1 cells arrest over and transmigration (as percentage of WT) across an MHEC monolayer under 0.8 dyne/cm$^2$ shear force. The photomicrographs show a representative DIC field at 200×. White triangles depict representative WT Th1 cell that arrested and polarized on VCAM-1 (*C*) and that adhered to and spread on ICAM-1 (*D*) or MHEC (*E*). Black triangles refer to representative Th1 CIP4$^{-/-}$ cells that kept rolling on VCAM-1 (*C*) and that adhered to but poorly spread on ICAM-1 (*D*) or MHEC (*E*). Results represent data from two independent experiments, with T cells from two mice used in each group. Error bars represent mean ± SEM. $^*P < 0.05$, $^{**}P < 0.01$.

## Discussion

This study demonstrates that the F-BAR domain-containing protein CIP4 is essential for optimal GC formation, skin inflammation, and integrin-dependent T-cell migration.

CIP4$^{-/-}$ mice had normal T- and B-cell development, their T cells proliferated, secreted cytokines, and expressed CD40L normally in response to TCR ligation, and their B cells proliferated and secreted IgG1 normally in response to LPS and CD40 ligation. However, their IgG and IgE antibody responses, high-affinity IgG antibody production in response to immunization with TD antigens were impaired, whereas their response to TI antigens was normal, suggesting a defect in in vivo T–B cell interaction. Migration of helper T cells into the B cell follicles is essential for driving GC formation (13), and integrin-mediated adhesion plays an important role in GC formation and TD antibody responses (14, 15). The number and the size of GCs were smaller in CIP4$^{-/-}$ mice than WT controls, but the density of CD3$^+$ T cells in the GCs was comparable. This is consistent with T cells in CIP4$^{-/-}$ mice being less efficient in entering follicles to nucleate GC formation. We cannot rule out a defect in the migration of antigen-activated B cells into the GCs of these mice.

CHS was severely impaired in CIP4$^{-/-}$ mice. Adoptive transfer studies revealed that the defect was intrinsic to the T cells. CD4$^+$ effector T cells from CIP4$^{-/-}$ mice were impaired in their ability to accumulate at sites of cutaneous antigen challenge and in intregrin-mediated TEM. Given the fact that integrins are important for the effector phase of CHS (16), it is likely that the impaired CHS in CIP4$^{-/-}$ mice was due, at least in part, to defective migration of effector T cells, which include CD4$^+$ and CD8$^+$ T cells. Impaired CHS was not due to defective T-cell proliferation to antigen, impaired survival, or decreased expression of skin homing receptors. However, defective retention of T cells in the skin cannot be ruled out.

T-cell tethering and rolling on both E- and P-selectin–coated surfaces were normal in the absence of CIP4. LFA1-mediated potentiation of T cell migration under static conditions was preserved in CIP4$^{-/-}$ T cells, suggesting that CIP4 may not be essential for TCR-mediated activation of integrins. In contrast, T-cell adhesive interactions with immobilized VCAM-1 and ICAM-1 under physiologic shear flow conditions showed striking defects. More importantly, CIP4$^{-/-}$ T cells were impaired in adhesion to, spreading on, and transmigration across a TNF-α–activated endothelial cell monolayer, a scenario that mimics the egress of effector T cells from blood vessels into inflamed tissue. These results suggest that CIP4 is important for the strength of integrin-dependent adhesive structures and their resistance to shear flow.

WASP is important for integrin-mediated cell adhesion (17, 18), and T cells from WAS patients show defective TEM (9). Through its association with WASP and WAVE proteins, CIP4 could be important in linking activated integrins, via their activation of Rho GTPases, to the actin cytoskeleton (19). Integrin linkage to the actin cytoskeleton inhibits the retrograde flow of actin and promotes integrin-mediated cell spreading and migration (20). A role for the CIP4/WASP complex in integrin-mediated Cdc42-dependent adhesion is supported by the observation that macrophages microinjected with CIP4 constructs deficient in either the microtubule- or the WASP-binding domain fail to assemble podosomes, adhesive structures that are also dependent on WASP (7, 21). Whereas podosomes have not been identified in T cells, podosome-like structures have been observed in T cells and may be important for cell adhesion and TEM (22, 23). Unlike its interacting partner WASP (24), CIP4 is not critical for TCR-mediated F-actin polymerization. TCR li-

gation caused increased F-actin content, capping of the TCR/CD3 complex, and spreading over anti-CD3–coated plates that were comparable in CIP4$^{-/-}$ and WT T cells.

The observation that CIP4, a member of the family of F-BAR domain containing proteins, plays a nonredundant role in T-cell trafficking to tissues suggests that CIP4 antagonists might be useful in treating T cell-mediated diseases by inhibiting the entry of effector T cells into target organs.

## Materials and Methods

**Generation of CIP4-Deficient Mice.** CIP4$^{-/-}$ mice were generated as detailed in the legend of Fig. S1. WT C57BL6 and OT-II mice were from Jackson Labs. All mice were kept in a pathogen-free environment. Procedures were performed in accordance with the Animal Care and Use Committee of the Children's Hospital Boston.

**FACS Analysis.** Single-cell suspensions from 8- to 12-wk-old mice were stained with PE- or FITC-labeled mAbs and analyzed on a FACS Canto (BD). Mabs to CD3ε, CD4, CD8, B220, IgM, CD43, CXCR4, CCR7, CD40L, LFA-1, Thy1.1, Thy1.2, CD44, and CD62L were from eBioscience; CD40, CD25, VLA-4, Fas, and GL-7 from BD Pharmingen. Rat mAb to CCR4, produced by L.K., recognizes T cells from WT, but not CCR4$^{-/-}$ mice and was used with DyLight 488 F(ab')$_2$ goat anti-rat IgG (Jackson ImmunoResearch). E-ligand was stained with mouse CD62E/Fc chimera (R&D Systems), with addition of EDTA as negative control.

**Purification and Activation of Splenic T and B Cells, Measurement of Antibody Responses, and GCs.** Assays for proliferation, cytokine production. antibody levels, affinity maturation, and GC formation have been previously published (25) and/or are detailed in *SI Materials and Methods*.

**CHS and Adoptive Transfer of CHS.** CHS to oxazolone and dinitrofluorobenzene (DNFB) was performed as in ref 26. and further detailed in *SI Materials and Methods*. For adoptive transfer, $25 \times 10^6$ cells taken from LN 5 d after sensitization, were injected i.v. in naïve recipients. Recipients were challenged 24 h later with hapten. Q-PCR was performed on skin samples using β2-microglobulin as a control.

**Adoptive Transfer of Activated OT-II Cells and Skin Challenge with OVA.** Adoptive transfer was performed as described (27). Splenic CD3$^+$ cells from OT-II Thy1.2 mice were activated in vitro for 5 d with irradiated WT splenocytes, 200 μg/mL OVA protein, and 10 ng/mL IL-2. CD4$^+$ cells were then purified and $6 \times 10^6$ cells were transferred to naïve Thy1.1 recipients, which were challenged the same day by i.d. injection in the ear of 10 μL of a 1:1 mixture of 25 μg of $OVA_{323–339}$ peptide in PBS and IFA. A 1:1 PBS + IFA mixture was used as control. Seven days later, single cell suspensions were prepared from the ears and stained for CD4 and Thy1.2.

**T-Cell Chemotaxis to SDF-1α.** Chemotaxis to SDF-1α across noncoated 5-μM filters for 2 h or 3-μM filters coated with sICAM-1 at 40 μg/mL for 30 min was performed as in ref 12.

**Th1 Cell Adhesion and Transmigration Assays Across Murine Heart Endothelial Cells (MHECs).** Th1 cell generation and TEM assays were performed as previously described (28, 29) and further detailed in *SI Materials and Methods*.

**Statistical Analysis.** Statistical analysis of the data using Student's *t* test or one-way or two-way ANOVA for multiple groups was performed with Prism software.

**ACKNOWLEDGMENTS.** This work was supported by US Public Health Service Grants HL059561, DK087348, CA131152, AI079769, AR052810, AI41707, and AI070085, the Roche Foundation (871233402), American Heart Association (2130011), and the Eleanor and Miles Shore Fellowship (to L.K.).

1. Heath RJ, Insall RH (2008) F-BAR domains: Multifunctional regulators of membrane curvature. *J Cell Sci* 121:1951–1954.
2. Aspenström P (1997) A Cdc42 target protein with homology to the non-kinase domain of FER has a potential role in regulating the actin cytoskeleton. *Curr Biol* 7: 479–487.
3. Tian L, Nelson DL, Stewart DM (2000) Cdc42-interacting protein 4 mediates binding of the Wiskott-Aldrich syndrome protein to microtubules. *J Biol Chem* 275:7854–7861.
4. Zimmerberg J, Kozlov MM (2006) How proteins produce cellular membrane curvature. *Nat Rev Mol Cell Biol* 7:9–19.
5. Hu J, et al. (2009) F-BAR-containing adaptor CIP4 localizes to early endosomes and regulates epidermal growth factor receptor trafficking and downregulation. *Cell Signal* 21:1686–1697.
6. Feng Y, et al. (2010) The Cdc42 interacting protein 4 (CIP4) gene knockout mouse reveals delayed and decreased endocytosis. *J Biol Chem* 285:4348–4354.
7. Linder S, Hüfner K, Wintergerst U, Aepfelbacher M (2000) Microtubule-dependent formation of podosomal adhesion structures in primary human macrophages. *J Cell Sci* 113:4165–4176.
8. von Andrian UH, Mackay CR (2000) T-cell function and migration. Two sides of the same coin. *N Engl J Med* 343:1020–1034.
9. Carman CV, et al. (2007) Transcellular diapedesis is initiated by invasive podosomes. *Immunity* 26:784–797.
10. MacLennan IC (2005) Germinal centers still hold secrets. *Immunity* 22:656–657.
11. Gorbachev AV, Fairchild RL (2001) Regulatory role of CD4+ T cells during the development of contact hypersensitivity responses. *Immunol Res* 24:69–77.
12. Park EJ, et al. (2007) Aberrant activation of integrin alpha4beta7 suppresses lymphocyte migration to the gut. *J Clin Invest* 117:2526–2538.
13. King C (2009) New insights into the differentiation and function of T follicular helper cells. *Nat Rev Immunol* 9:757–766.
14. Ochs HD, Nonoyama S, Farrington ML, Fischer SH, & Aruffo A (1993) The role of adhesion molecules in the regulation of antibody responses. *Semin Hematol* 30 (4 Suppl 4):72–79.
15. Cannons JL, et al. (2010) *Optimal Germinal Center Responses Require A Multistage T Cell:B Cell Adhesion Process Involving Integrins, SLAM-Associated Protein, and CD84* (Immunity).
16. Scheynius A, Camp RL, Puré E (1996) Unresponsiveness to 2,4-dinitro-1-fluoro-benzene after treatment with monoclonal antibodies to leukocyte function-associated molecule-1 and intercellular adhesion molecule-1 during sensitization. *J Immunol* 156: 1804–1809.
17. Zhang H, et al. (2006) Impaired integrin-dependent function in Wiskott-Aldrich syndrome protein-deficient murine and human neutrophils. *Immunity* 25:285–295.
18. Tsuboi S, Nonoyama S, Ochs HD (2006) Wiskott-Aldrich syndrome protein is involved in alphaIIb beta3-mediated cell adhesion. *EMBO Rep* 7:506–511.
19. Deakin NO, et al. (2009) An integrin-alpha4-14-3-3zeta-paxillin ternary complex mediates localised Cdc42 activity and accelerates cell migration. *J Cell Sci* 122: 1654–1664.
20. Vicente-Manzanares M, Choi CK, Horwitz AR (2009) Integrins in cell migration—the actin connection. *J Cell Sci* 122:199–206.
21. Tsuboi S, et al. (2009) FBP17 mediates a common molecular step in the formation of podosomes and phagocytic cups in macrophages. *J Biol Chem* 284:8548–8556.
22. Carman CV (2009) Mechanisms for transcellular diapedesis: Probing and pathfinding by 'invadosome-like protrusions'. *J Cell Sci* 122:3025–3035.
23. Evans R, et al. (2009) Integrins in immunity. *J Cell Sci* 122:215–225.
24. Snapper SB, et al. (1998) Wiskott-Aldrich syndrome protein-deficient mice reveal a role for WASP in T but not B cell activation. *Immunity* 9:81–91.
25. Jabara H, et al. (2002) The binding site for TRAF2 and TRAF3 but not for TRAF6 is essential for CD40-mediated immunoglobulin class switching. *Immunity* 17:265–276.
26. Martin SF, et al. (2008) Toll-like receptor and IL-12 signaling control susceptibility to contact hypersensitivity. *J Exp Med* 205:2151–2162.
27. McLachlan JB, Catron DM, Moon JJ, Jenkins MK (2009) Dendritic cell antigen presentation drives simultaneous cytokine production by effector and regulatory T cells in inflamed skin. *Immunity* 30:277–288.
28. Alcaide P, et al. (2007) The 130-kDa glycoform of CD43 functions as an E-selectin ligand for activated Th1 cells in vitro and in delayed-type hypersensitivity reactions in vivo. *J Invest Dermatol* 127:1964–1972.
29. Lim YC, et al. (2003) Heterogeneity of endothelial cells from different organ sites in T-cell subset recruitment. *Am J Pathol* 162:1591–1601.